Transient Stable Corrective Control Using Neural Lyapunov Learning

Bellizio, Federica; Cremer, Jochen L.; Strbac, Goran

DOI
10.1109/TPWRS.2022.3204459

Publication date
2022

Document Version
Final published version

Published in
IEEE Transactions on Power Systems

Transient Stable Corrective Control Using Neural Lyapunov Learning

Federica Bellizio, *Student Member, IEEE*, Jochen L. Cremer, *Member, IEEE*, and Goran Strbac, *Member, IEEE*

***Abstract*—This paper proposes a method to compute corrective control actions for dynamic security in real-time and quantifies the economic value of corrective control. Lowered inertia requires fast control methods in real-time to correct system operation and maintain system security when equipment fails. However, using corrective control beyond such emergency failure measures does not make fully use of them. The key contribution of this work is the optimal use of corrective control applications in combination with preventive strategies to enhance the network utilisation, reduce the normal operating costs while maintaining adequate security levels. The proposed approach learns a neural network for safety certificates and models the predicted safe dynamic post-fault state as algebraic constraints in an AC optimal power flow (OPF) deciding close to real-time on the optimal corrective control. Considering these safety constraints within the ACOPF can balance simultaneously the system transient stability with the costs for preventive and corrective control. This proposed approach outperforms sub-optimal approaches aiming at sequentially finding the balance. Case studies were based on the IEEE 9-bus system with integrated electrical vehicles and shares of wind power up-to 40% and on the IEEE 39-bus and 118-bus systems. The proposed approach outperforms baseline control approaches in stability, economics, and carbon emissions. One baseline approach was preventive wind curtailment, against which the proposed approach reduced operating costs by up-to 60%, decreased unstable operations by 50% and reduced carbon emissions by 60% in the IEEE 9-bus. In the IEEE 39-bus and 118-bus systems, the approach was promising for larger systems.**

***Index Terms*—Neural networks, lyapunov functions, optimal power flow, transient stability assessment, corrective control.**

I. Introduction

MODERN operations of electric power systems undergo significant changes. The high share of renewable and distributed energy resources (DERs) makes the generation and demand more uncertain and barely predictable compared to the past. In addition to the difficulty in predicting renewable power outputs, DERs are integrated into the system through power electronic devices. These converter-interfaced generating (CIG) devices are fast-acting controllers and do barely supply inertia to the system. A low-inertia system has faster dynamics (e.g. in the timescales of electromagnetic waves) which challenges stable operations after an unforeseen system fault [1], [2]. Operators can prevent possible upcoming system instabilities if they are known in advance. However, these instabilities are little known in the future due to the difficulty in predicting renewable system operations. To still keep the system stable, the current strategies are either considering more conservative preventive measures or investing in new system infrastructure. These two strategies are costly and inefficient [3].

Corrective control is an alternative strategy for efficiently and cheaply ensuring stable normal operations [4], [5]. Corrective control adjusts system 'post-fault' operation in response to a disturbance or a fault. Currently, corrective control is only used for emergency responses, and an example of control action is load shedding. A promising opportunity is to use corrective control also in normal operations leveraging the new technological advantages of very fast-acting (corrective) CIG controllers. However, a research gap is a control method that can compute optimal corrective control measures for real-time considering the system stability in normal operations.

It is challenging to consider corrective control in real-time system operation. The system operation can be modelled as a nonlinear AC optimal power flow (ACOPF) optimisation which can consider preventive control. However, the ACOPF cannot consider corrective control easily. Considering corrective control requires modeling post-fault system states and corresponding post-fault decisions in the optimisation. The post-fault dynamics are highly nonlinear differential-algebraic equations (DAE) which require to model transient constraints in the optimisation. Modelling such constraints makes the ACOPF optimisation very slow. This is challenging as ideally the ACOPF would be solved every five minutes to account for rapid fluctuations of demand and generation, but this is infeasible in real-time.

Approaches to consider corrective control in real-time operation can either aim at predicting operation decisions with machine learning (ML) instead of solving the optimisations or aim at finding approximations for transient constraints for the ACOPF. As solving the ACOPF in real-time is not possible, recently, ML models are designed to predict the ACOPF solution. For example, artificial neural networks (NNs) can either directly predict the optimal solution [6] or classification and regression models can predict the economic OPF costs [7], however, these approaches do not predict transients and are not developed yet for corrective control. Numerical approaches (Forward Euler or

Manuscript received 29 November 2021; revised 22 March 2022 and 8 June 2022; accepted 28 August 2022. Date of publication 5 September 2022; date of current version 22 June 2023. Paper no. TPWRS-01813-2021. *(Corresponding author: Federica Bellizio.)*

Federica Bellizio and Goran Strbac are with the Electrical & Electronic Engineering, Imperial College London, SW7 2AZ London, U.K. (e-mail: f.bellizio18@imperial.ac.uk; g.strbac@imperial.ac.uk).

Jochen L. Cremer is with the Electrical Sustainable Energy, Delft University of Technology, 2628 Delft, The Netherlands (e-mail: j.l.cremer@tudelft.nl).

Color versions of one or more figures in this article are available at https://doi.org/10.1109/TPWRS.2022.3204459.

Digital Object Identifier 10.1109/TPWRS.2022.3204459

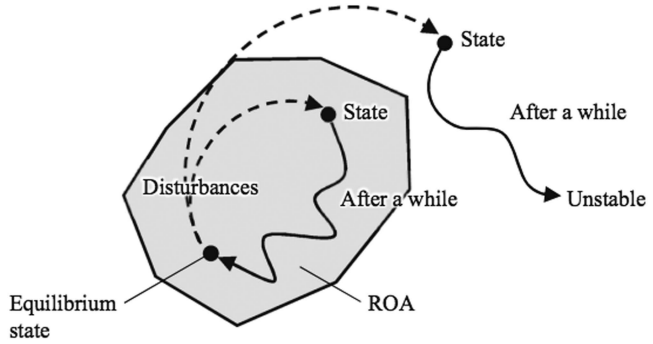

Fig. 1. Definition of region of attraction [16].

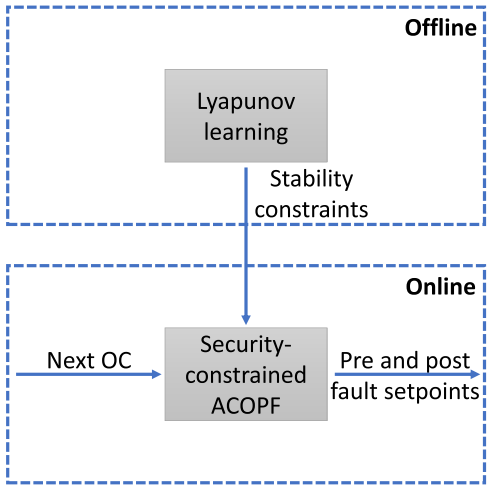

Fig. 2. The proposed control approach for security-constrained ACOPF.

Runge-Kutta) can compute the exact transients from the DAEs which are computationally hard above all in large systems. Approximations of the transients for ACOPFs can be easier computed through heuristics, discretisations, simplifications, or energy functions [8], [9]. Heuristics connect the ACOPF optimiser with a simulator. The ACOPF generation dispatch is simulated for dynamic stability [5], and when found unstable, the dispatch is modified until the system stabilises. NNs can be also used to substitute dynamic simulations in some iterations as in [10]. Another approach discretises the DAEs in time [11], [12] and considers the discretised transient constraints in the ACOPF which can result in many constraints and significantly slows down ACOPFs in larger systems. The single-machine equivalent (SIME) approach [13] simplifies the dynamical model. However, the simplified stability limits for each generator cannot consider coupling effects. Another approach uses energy functions and derives the certification of safety [14], [15]. The energy functions can be used as Lyapunov functions and the sublevel sets of these functions as region of attraction (ROA in Fig. 1) that represents the subspace of all operating states converging to a steady-state equilibrium [16]. The ROA can be a security constraint for the ACOPF. This approach does not require computing the full system transients, results in low computational cost, however, is only applicable for very simple systems. Unfortunately, all of the aforementioned approaches are unsuitable for real-time corrective control as they either cannot consider corrective actions or are too slow for real-time.

Recently, a novel approach from ML seems promising to address a key issue in identifying Lyapunov functions. The key issue of the Lyapunov function based approach is to identify the function for large and complex systems [17]. Particularly, for complex dynamical systems such as power systems the functions are very hard to find [18]. For instance, a semi-definite program is efficient only when the dynamics are polynomial and the Lyapunov function is restricted to be a sum-of-squares polynomial [16]. However, assuming linear or polynomial approximations pose much restriction on the system and the Lyapunov function. Recently, in ML research, NNs seems suitable to model the Lyapunov function and avoid linear or polynomial approximations [19], [20], [21]. In [22], a NN learns the control law and the Lyapunov function that maximise the ROA of a general nonlinear dynamical system. The learner uses stochastic gradient descent to find the optimal parameters of the control law and the neural Lyapunov function that minimises the Lyapunov risk. This risk measures the violations of the Lyapunov conditions. This NN-based approach can assess the transient stability of power systems in [23], [24], [25], however, this approach was never used to consider the system's transient response within the ACOPF.

A. Proposed Approach

This paper proposes the NN-LYAPUNOV CONTROL approach, an OPF-based optimisation that considers NN-trained ROAs as stability constraints and preventive and corrective control as decisions. The flowchart of the proposed control approach is shown in Fig. 2. The NN training approach transforms offline the differential and nonlinear constraints for transient post-fault stability into algebraic constraints which are manageable by the OPF optimisation. The OPF is then solved online for each next operating condition (OC) to obtain the optimal pre- and post-fault setpoints. The proposed NN-LYAPUNOV CONTROL estimates and maximises the ROA of the post-fault system [22] resulting in highly efficient corrective and preventive control actions. The contribution of this work is threefold:

1) Deriving algebraic stability constraints for the post-fault system using NN-based Lyapunov functions. The NNs learn the optimal controller and the Lyapunov function to obtain larger ROAs compared against standard control methods. This optimises the balance of transient stability and economic cost.
2) Considering the system's transient response within the OPF using the derived algebraic constraints. The DAEs for transient stability are transformed into algebraic operational constraints using the learned ROA for the post-fault system. This results in transient stable, cost-optimal post-fault operating conditions.
3) Using corrective control not only as a backup strategy but as an active role in maintaining the system stability.

This reduces operational costs and carbon emissions while maintaining adequate levels of stability.

A case study tested the approach on the IEEE 9-bus system with integrated DERs for two scenarios, for 25% of renewable sources and for 40% of renewable sources. The scenarios considered wind farms and fleets of electrical vehicles (EVs) with vehicle-to-grid (V2G) technology as corrective control. The study compares the approach against baselines such no control, only preventive control and ML-based corrective control. Case studies on the IEEE 39-bus and 118-bus systems finally tested the stability performance of the proposed approach on large systems. The rest of this paper is structured as follows. Section II introduces the dynamical model of power systems. Thereafter, Sections III-IV describe the neural learning of the Lyapunov function and the implementation of the transient constraints within the ACOPF. Subsequently, Section V presents the case study and Section VI finally draws the conclusions.

II. Power System's Dynamics

The classical model of a multimachine system is used [26]. Let N be the number of buses, ε the set of transmission lines, B_{ij} the susceptance matrix of lines $(i,j) \in \varepsilon$, G the set of synchronous generator buses and B the set of load buses. In this model, the loads are represented by passive impedances and the mechanical power $P_{m,i}$ for each generator bus $i \in G$ is assumed constant over the timescale of transients. The Kron reduced model is used to aggregate the load buses into generator buses. Each generator bus has the conventional momentum of inertia $M_i = \dfrac{\omega_R}{2H_i}$ where H_i is the inertia and ω_R the frequency reference, and the damping factor D_i. The dynamical model of a multimachine system is a second order nonlinear and differential equation, also known as swing equations:

$$\begin{aligned} \dot{\delta}_i &= \omega_i, \ \forall i = 1 \ldots |G| \\ M_i \dot{\omega}_i &= P_{m,i} - \sum_{j=1, j \neq i}^{N} B_{i,j} \sin(\delta_i - \delta_j), \ \forall i = 1 \ldots |G| \end{aligned} \tag{1}$$

with δ_i and ω_i the phase angle and frequency at each generator bus i. The transient stability is then assessed using the Integral Square Generator Angle (ISGA) index that is defined as follows [27]:

$$\begin{aligned} \delta_{coak} &= \frac{1}{M_{tot}} \sum_{i \in G} M_i \delta_{i,k}, \ \forall k = 0, \ldots T \\ J_k &= \frac{1}{M_{tot}} \sum_{i \in G} M_i (\delta_{i,k} - \delta_{coak})^2, \ \forall k = 0, \ldots T \\ \bar{J} &= \frac{1}{|T|} \sum_{k=0, \ldots T} J_k \end{aligned} \tag{2}$$

where δ_{coak} is the centre of angle at the time step k and $M_{tot} = \sum_{i \in G} M_i$ is the total inertia. The ISGA index $\bar{J}$ is the time-average of the element-wise J_k. Higher values of $\bar{J}$ correspond to unstable operating conditions following a disturbance.

III. Learning the Lyapunov Function for Stability

The key role of the ROA in power system stability is described in the following transient stability problem (adapted from [28]). Suppose that at time t_0 the power system is subjected to a severe transient disturbance (fault), e.g. a short circuit. During the fault, the system responds by large excursions of the system variables. At t_1 the fault is cleared, the system reaches a new state $x_1(t_1)$ and switches to post-fault system. The transient stability problem considers whether the trajectory $x(t \geq t_1)$ with initial conditions $x(0) = x_1(t_1)$ will converge to an asymptotically stable equilibrium point. The system will return to steady-state operation only if $x_1(t_1)$ belongs to the ROA of the post-fault steady-state. Hence, the larger the ROA, the more operating conditions can reach post-fault stability, and a system with large ROA can be considered robust against large disturbances.

Several approaches can estimate the ROA of a generic nonlinear system such as the power system. A straightforward approach is to use time-domain simulations to check every point in the neighborhood of the stable equilibrium point. This approach provides the exact ROA but is impractical for large-scale systems due to high computational costs and does not provide any closed form for control design purposes meaning that it does not allow to enlarge the ROA. More promising is the approach based on Lyapunov functions where the sublevel sets of these functions estimate the ROA. The corresponding training of the NN to identify the optimal controller and Lyapunov function is described [22].

Given the system's dynamics $(\dot{\delta}, \dot{\omega}) = f_u(\delta, \omega)$ described in (1) with controller $u = P_m$ and state $x = (\delta, \omega)$, a Lyapunov function V can be used to establish the stability of the post-fault state $x^* = (\delta^*, \omega^*)$ as follows:

Definition 1: If in a ball $D_R = \{x | ||x||_2^2 \leq R^2\}$ with radius R, there exist a continuous differentiable scalar function V such that:

1) V is positive definite in D_R
2) $\dot{V} = \dfrac{dV(x(t))}{dt} = \mathcal{L}_{f_u} V(x(t))$ is negative definite in D_R

then $x^* = (\delta^*, \omega^*)$ is asympotically stable and V is a Lyapunov function.

The sublevel set of the Lyapunov function $S_c \, \forall c \geq 0$ is defined as

$$S_c = \{x \in D_R | V(x) \leq c\} \tag{3}$$

and can be used to approximate the ROA. The ROA is an invariant subset such that all system trajectories starting inside this subset asymptotically converge back to the post-fault state. For a state deviation from x^* falling within the ROA, the system can be assessed to be stable as the system trajectories resulting from the deviation will converge back to x^*. Therefore, the ROA can be used to certify the stability of the post-fault state as long as a Lyapunov function for the post-fault system can be identified.

A multilayered feedforward NN with $tanh$ activation function is assumed as structure of the Lyapunov function. The learning framework, shown in Fig. 3, is an unsupervised learning task that is composed of a learner and a falsifier. Using u to denote both the NN parameters and the controller, the learning module

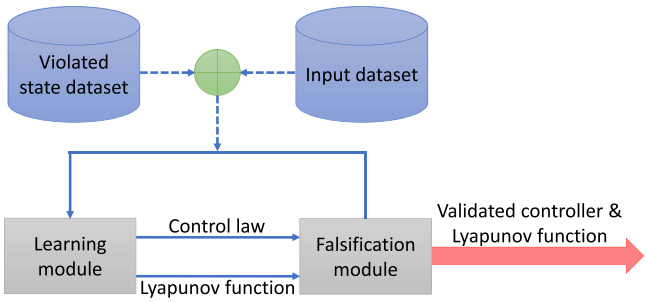

Fig. 3. The neural learning of the optimal controller and Lyapunov function.

updates u to improve the likelihood to satisfy the Lyapunov conditions that are formulated as a cost function also named the Lyapunov risk. The Lyapunov risk measures the degree of violation of the following conditions: i) $V_u(x)$ is positive, ii) $\mathcal{L}_{f_u}V_u(x)$ is negative, iii) $V_u(x^*)=0$. Therefore, the design objective is to minimise the following Lyapunov risk $L(u)$ by updating the controller and parameters u:

$$L(u)=\frac{1}{N}\sum_{k=1}^{N}(\max(0,-V_u(x_k))+\max(0,\mathcal{L}_{f_u}V_u(x_k))) + V_u^2(x^*)+\beta \tag{4}$$

where N is the number of training samples and β is the cost term that regulates how quickly the Lyapunov function value increases with respect to the radius of the level sets:

$$\beta := \frac{1}{N}\sum_{k=1}^{N}||x_k||_2 - \alpha V_u(x_k) \tag{5}$$

where α is a tunable parameter. The cost term β allows to adjust the controller and the NN parameters u to maximise the corresponding ROA of the learned Lyapunov function. The parameters u are initiated to the linear quadratic regulator (LQR) solution that is obtained by linearising the dynamics in a small neighborhood of the origin [29].

As a second step of the diagram in Fig. 3, for each learned controller and Lyapunov function pair (V_u, u), there is a falsifier that finds the states violating the Lyapunov conditions, also called counterexamples, and these counterexamples are then added to the training set for the next learning step. The falsification constraints are defined as follows:

$$\Phi_\varepsilon(x) := \left(\sum_{k=1}^{N}x_k^2 \geq \varepsilon\right) \wedge \left(V_u(x)\leq 0 \vee \mathcal{L}_{f_u}V_u(x)\geq 0\right) \tag{6}$$

where ε is a positive constant parameter that bounds the tolerable numerical error. This parameter allows to avoid numerical issues as values within the ball with radius ε are physically insignificant and does not affect the learned Lyapunov function. To solve the falsification constraints that would require the minimisation of highly nonconvex functions, the SMT solver dReal based on the δ-completeness property is used [30]. When the δ-complete algorithm concludes that (6) is unsatisfiable, then the Lyapunov conditions hold for all states, otherwise counterexamples are obtained and added to the training set. The learning stops when no counterexamples are found. The outputs of the neural learning are the parameters u of the validated Lyapunov function V_u and the weight matrix W of the corresponding optimal controller $u=g(x)=W\cdot x$.

Once the NN Lyapunov function for the post-fault system is learned, the corresponding ROA provides bounds for the maximum state deviation for which the system trajectories are bounded within the ROA and asymptotically converge to the origin. In the steady-state post-fault system $\omega=\dot{\delta}=0$, then the lower bound in the state space is $\delta_{\min}=(\delta,\omega=0)\in S_{c_0}$ with $S_{c_0}=\{S_c|c=0\}$ such that

$$\sum_{i=1}^{|G|}|\delta_i-\delta_{i,\min}|^2 \text{ is minimised} \tag{7}$$

where $\delta_{i,\min}=\min\{\delta_i:(\delta,\omega=0)\in S_{c_0} \wedge \delta_{j\neq i}=0\}$. Similarly, the upper bound in the state space is $\delta_{\max}=(\delta,\omega=0)\in S_{c_0}$ such that

$$\sum_{i=1}^{|G|}|\delta_i-\delta_{i,\max}|^2 \text{ is minimised} \tag{8}$$

where $\delta_{i,\max}=\max\{\delta_i:(\delta,\omega=0)\in S_{c_0} \wedge \delta_{j\neq i}=0\}$. Finally, the bounds in the input space can be easily derived as $u_{\min}=g(\delta_{\min},\omega=0)$ and $u_{\max}=g(\delta_{\max},\omega=0)$ and used as operational constraints in the following optimisation problem.

IV. Stability Constrained ACOPF

This section formulates the optimisation problem to identify a feasible operating condition that fulfills all power network constraints in the pre-fault state and the power networks and stability constraints in the post-fault state. The subscripts p and P are used to differentiate the pre-fault and the post-fault variables, respectively. The objective function is the minimisation of the operational costs and hence of the pre-dispatched generation costs. No costs are assumed for corrective control following the fault. The proposed optimisation problem is a modification of a relaxed ACOPF formulation that uses the Semi Definite Programming (SDP) relaxation and efficiently finds a global optimal solution [31]. This modification minimises the mean squared distance from a predicted generator dispatch $[\hat{P}_{G_i},\hat{Q}_{G_i}]$ to a feasible generator dispatch $[P_{G_i,p},Q_{G_i,p}]$. These mean squared differences in the pre-fault active and reactive powers are α_i and γ_i for generator $i\in G$. Then, the full optimisation problem is:

$$\min \sum \alpha_i+\lambda\gamma_i \tag{9a}$$

subject to

$$P_{G_i,P}=P_{G_i,p}+\Delta P_{G_i} \quad \forall i\in G \tag{9b}$$

$$P_{G_i}^{\min}\leq P_{G_i,p}\leq P_{G_i,p}^{\max} \quad \forall i\in G \tag{9c}$$

$$Q_{G_i}^{\min}\leq Q_{G_i,p}\leq Q_{G_i,p}^{\max} \quad \forall i\in G \tag{9d}$$

$$u_{\min}\leq \Delta P_{G_i}\leq u_{\max} \quad \forall i\in G \tag{9e}$$

$$-P_{Db}+\sum_{i\in G}P_{G_i,p}=\text{tr}(\mathbf{Y}_{b,p}\mathbf{W}_p)\quad\forall b\in B \tag{9f}$$

$$-P_{Db}+\sum_{i\in G}P_{G_i,P}=\text{tr}(\mathbf{Y}_{b,P}\mathbf{W}_P)\quad\forall b\in B \tag{9g}$$

$$-Q_{Db}+\sum_{i\in G}Q_{G_i,p}=\text{tr}(\bar{\mathbf{Y}}_{b,p}\mathbf{W}_p)\quad\forall b\in B \tag{9h}$$

$$-Q_{Db}+\sum_{i\in G}Q_{G_i,P}=\text{tr}(\bar{\mathbf{Y}}_{b,P}\mathbf{W}_P)\quad\forall b\in B \tag{9i}$$

$$(V_b^{\min})^2\le\text{tr}(\mathbf{M}_{b,p}\mathbf{W}_p)\le(V_b^{\max})^2\quad\forall b\in B \tag{9j}$$

$$(V_b^{\min})^2\le\text{tr}(\mathbf{M}_{b,P}\mathbf{W}_P)\le(V_b^{\max})^2\quad\forall b\in B \tag{9k}$$

$$\begin{bmatrix}-(S_k^{\max})^2 & \text{tr}(\mathbf{Z}_{kl}\mathbf{W}_p) & \text{tr}(\bar{\mathbf{Z}}_{kl}\mathbf{W}_p)\\ \text{tr}(\mathbf{Z}_{kl}\mathbf{W}_p) & -1 & 0\\ \text{tr}(\bar{\mathbf{Z}}_{kl}\mathbf{W}_p) & 0 & -1\end{bmatrix}\le 0\qquad\forall k\in\varepsilon \tag{9l}$$

$$\begin{bmatrix}-(S_k^{\max})^2 & \text{tr}(\mathbf{Z}_{kl}\mathbf{W}_P) & \text{tr}(\bar{\mathbf{Z}}_{kl}\mathbf{W}_P)\\ \text{tr}(\mathbf{Z}_{kl}\mathbf{W}_P) & -1 & 0\\ \text{tr}(\bar{\mathbf{Z}}_{kl}\mathbf{W}_P) & 0 & -1\end{bmatrix}\le 0\forall k\in\varepsilon \tag{9m}$$

$$\begin{bmatrix}-(S_k^{\max})^2 & \text{tr}(\mathbf{Z}_{km}\mathbf{W}_p) & \text{tr}(\bar{\mathbf{Z}}_{km}\mathbf{W}_p)\\ \text{tr}(\mathbf{Z}_{km}\mathbf{W}_p) & -1 & 0\\ \text{tr}(\bar{\mathbf{Z}}_{km}\mathbf{W}_p) & 0 & -1\end{bmatrix}\le 0\quad\forall k\in\varepsilon \tag{9n}$$

$$\begin{bmatrix}-(S_k^{\max})^2 & \text{tr}(\mathbf{Z}_{km}\mathbf{W}_P) & \text{tr}(\bar{\mathbf{Z}}_{km}\mathbf{W}_P)\\ \text{tr}(\mathbf{Z}_{km}\mathbf{W}_P) & -1 & 0\\ \text{tr}(\bar{\mathbf{Z}}_{km}\mathbf{W}_P) & 0 & -1\end{bmatrix}\le 0\quad\forall k\in\varepsilon \tag{9o}$$

$$\begin{bmatrix}-\alpha_i & P_{G_i,p}-\hat{P}_{G_i}\\ P_{G_i,p}-\hat{P}_{G_i} & -1\end{bmatrix}\le 0\quad\forall i\in G \tag{9p}$$

$$\mathbf{W}_p\ge 0 \tag{9q}$$

$$\mathbf{W}_P\ge 0 \tag{9r}$$

where λ is a user-defined scaling parameter to cope with the different orders of magnitudes of α and γ. Pre- and post-fault active and reactive power injections P_{G_i}, Q_{G_i}, the post-fault ΔP_{G_i} and pre- and post fault voltage matrices $\mathbf{W_p}$ and $\mathbf{W_P}$ are the decision variables. Equation (9e) guarantees the post-fault state is transient stable with $u_{\min}$ and $u_{\max}$ the bounds introduced in Section III and ΔP_{Gi} the deviation from the pre-fault generator dispatch due to corrective control. All other parameters are introduced and better explained in [31]. The pre-fault voltage coordinates $w_p=[V_{d1,p},\dots V_{dN,p},V_{q1,p},..V_{qN,p}]$ with $V_{i,p}=V_{di,p}+V_{qi,p}$ the voltage phasor in rectangular coordinates, can be recovered through

$$\text{rank}(\mathbf{W}_p)=\text{rank}(w_p w_p^T)=1 \tag{10}$$

This optimisation is convex and can be solved with a second-order cone solver, e.g. Mosek, SCS [31]. The outputs are the optimised pre-fault generator dispatches (P_{Gi},Q_{Gi}), the generator bus voltages (V_{Gdi},V_{Gqi}) and the corrective power injections ΔP_{Gi} for each generator bus $i\in G$.

V. Case Study

This section provides a brief tutorial on the proposed approach to learn the Lyapunov based stability constraints, subsequently analyses the stability of the proposed approach and the reductions of economic costs and carbon emissions.

A. Test System and Assumptions

A modified version of the IEEE 9-bus system from [32] was used as test system in the following studies, unless indicated otherwise. The modification included integrated DERs, all lines had a minimum resistance of 10^{-4} p.u., a storage capacity of 20 MWh was available at each generator bus using EV fleets, and two scenarios with renewable sources were considered: a) 25% of fossil fuel generation was replaced by wind power, b) 40% of fossil fuel generation was replaced by wind power. Generation redispatch and energy storage using the EVs were considered for preventive and corrective control [33], respectively. 1000 load scenarios were sampled from a Latin hypercube with uniform distribution around $\pm 50\%$ of the nominal value for the active power and $\pm 20\%$ for the reactive power. A short circuit at bus 8 at time 0.1 s was considered as fault. The fault was then cleared at 0.25 s by opening the line between buses 8 and 9. Corrective control was applied only once the fault was cleared as there is always a latency of up to 0.25 s between the fault occurrence and the real activation of the corrective control due to communication delays. During the time interval $[0.1, 0.25]$s, transient assistive measures (TAMs) were applied [5]. These measures usually last for few milliseconds, so they are not optimised. The transient stability was analysed over a simulation time $T=10$ s and the optimal post-fault operating condition was then assessed as stable if the index ISGA ≤ 0.47, otherwise unstable [27]. 93% and 99% of OCs were unstable when no preventive and corrective control was applied at scenarios (a) and (b), respectively. These high rates of unstable OCs showed that high shares of renewable sources make the system strongly unstable.

The NN structure to learn the Lyapunov function had 3 linear layers, one input, one hidden with 6 neurons and one output layer, all using $tanh$ as activation function. 1000 training data $x_i=[\delta_1,\dots,\delta_{|G|},\dot{\delta}_1,\dots,\dot{\delta}_{|G|}]$, with $i=1\dots1000$ and $|G|=3$, were fed into the input layer. Each training data x_i was uniformly sampled between $[-1,1]$ p.u. corresponding to the maximum phase angle deviation $\pm 57^\circ$ from the initial pre-fault condition. The NN structure was implemented using the package PyTorch 1.7 with Python 3.8.5 [34]. The optimiser ADAMW was used with a learning rate of 0.01. Finally, the optimisation problem (9a)-(9r) was implemented in CVXPY 1.1.5 with $\lambda=100$ and solved using the SCS solver with default settings. The slack bus phase angles were set at 0° to get unique solutions to the optimisation. The time-domain simulations were then carried out in Matlab R2016a using a sixth stage-fifth order Runge-Kutta method (ode45 function).

The performance of the proposed approach was finally tested on larger systems using: (c) the IEEE 39-bus system with 10 machines and system parameters taken from [25], and (d) the IEEE 118-bus system with 19 machines and system parameters taken from [35]. In both systems, a storage capacity of 30 MWh was available at each generator bus using EV fleets. There, the NN to learn the Lyapunov function had 5 linear layers, with 4 nodes at each hidden layer. 500 load scenarios were sampled with uniform distribution around $\pm 5\%$ of the nominal value for the active and reactive power. The same transient assumptions of the IEEE 9-bus system were considered for these two larger systems. Short circuit faults were considered at buses 4 and 12 in (c) and (d), respectively.

B. Why NNs to Learn the Lyapunov Function

This study investigated the learning of the NN based Lyapunov function and compared the proposed approach with regards to stability and cost for preventive control against a more analytical learning approach for Lyapunov functions. The Lyapunov function for the post-fault system was learned by the

i) 3 layers feed-forward NN-LYAPUNOV approach (Section III)
ii) initial LQR LYAPUNOV controller approach.

The neural Lyapunov learning converged in 3110 iterations by setting the numerical error parameter $\varepsilon = 0.5$ and $\delta = 0.01$ for the falsification step. This learning procedures found a Lyapunov function that is proved to be valid within the region $||x||_2 \leq 1$ and the following optimal controller:

$$u = W \cdot x \tag{11}$$

with

$$u = [P_{m,1}, P_{m,2}, P_{m,3}]$$

$$x = [\delta_1, \delta_2, \delta_3, \dot{\delta_1}, \dot{\delta_2}, \dot{\delta_3}]$$

$$W = \begin{bmatrix} -0.102 & -0.469 & -0.256 & 0.021 & -0.217 & 0.231 \\ 0.108 & -0.342 & -0.247 & -0.736 & -0.152 & 0.056 \\ -0.287 & -0.504 & -0.195 & 0.109 & -0.216 & -0.615 \end{bmatrix} \tag{12}$$

The learned NN-based Lyapunov function is shown in Fig. 4 for the pair $(\delta_1, \dot{\delta}_1)$ with the dashed red circle defining the valid region. For both scenarios a) with 25% and b) with 40% wind power described in Section V-A, the Lyapunov function for the post-fault system was learned only once as the Lyapunov function is an invariant property of the nonlinear system itself, i.e. the conclusion of the system stability is independent from the initial conditions [36]. Therefore, the same Lyapunov function can be used to determine the stability region in both scenarios. The corresponding ROAs of the Lyapunov functions learned using (i)-(ii) are compared in Fig. 5. It resulted the NN learning allowed to significantly enlarge the ROA compared to the LQR solution. The larger ROA enhanced the balance between costs and system stability as shown below.

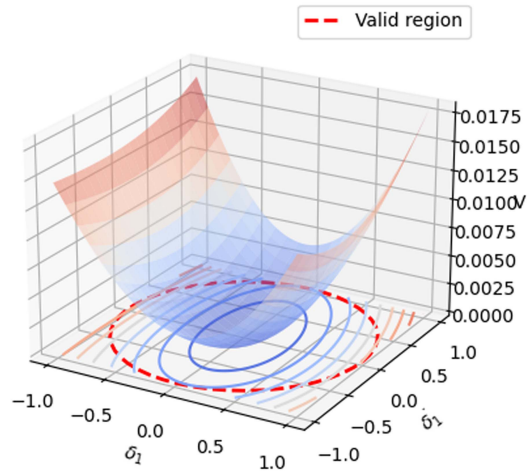

Fig. 4. Lyapunov function learned using the NN learning procedure.

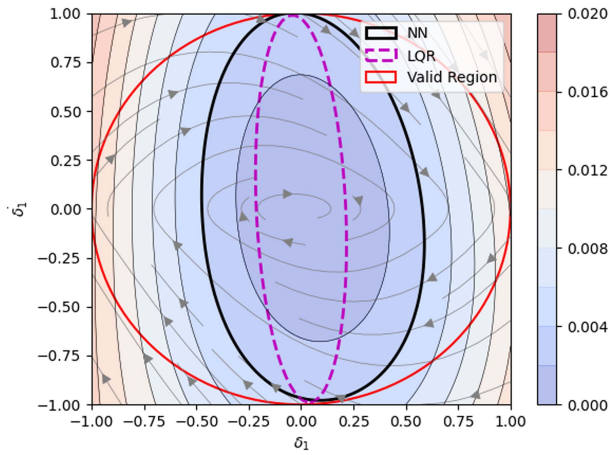

Fig. 5. ROAs estimated using different Lyapunov functions.

The stability bounds were obtained by setting $\dot{\delta}_i = 0$ as the post-fault operating condition is a steady-state condition with time derivatives of the generator phase angles equal to zero. These state-space bounds $(\delta_{\min,i}, \delta_{\max,i})$ were finally replaced in Eq. (11) to derive the corresponding bounds in the input space, $u_{\min} = [-18, -5, -29]$ MW and $u_{\max} = [18, 6, 27]$ MW, to be included in the ACOPF (9a)–(9r) as stability constraints. The need of a NN based learning for the optimal controller and Lyapunov function was investigated by comparing the approaches (i)-(ii) with regards to stability and cost of preventive control. The ACOPF was solved using the two stability constraints derived from the NN and the LQR based Lyapunov functions. Then, the fault was simulated using the optimal pre-fault generator dispatch as initial conditions and applying the optimised corrective power injections when the fault was cleared.

The stability and cost results for approaches (i)-(ii) are summarised in Table I for scenario (a)-(b) and compared against the baseline approach WIND CURTAIL. In the baseline approach, the wind power was curtailed and replaced by fossil fuel generation as preventive control without carrying out any optimisation. In this way, the system's inertia was increased to improve the

TABLE I
STABILITY AND COSTS OF NN AND LQR BASED LYAPUNOV FUNCTIONS WITH 25% (a) AND 40% (b) RENEWABLES

	Approaches		
	WIND CURTAIL	(i) NN LYAPUNOV	(ii) LQR LYAPUNOV
$(a)-Unstable\ OCs$	418/1000	0/1000	0/1000
$(a)-Cost\ reduction$	–	−2.7m (−48%)	−2.6m (−46%)
$(b)-Unstable\ OCs$	510/1000	0/1000	0/1000
$(b)-Cost\ reduction$	–	−3.7m (−62%)	−3.6m (−60%)

TABLE II
STABILITY AND COSTS OF THREE CONTROL APPROACHES WITH 25% (a) AND 40% (b) RENEWABLE INTEGRATION

	Approaches		
	PREVENTIVE CONTROL	DT CONTROL	LYAPUNOV CONTROL
$(a)-Unstable\ OCs$	23/1000	95/1000	0/1000
$(a)-Cost\ reduction$	−2m (−35%)	−3.1m (−54%)	−2.8m (−48%)
$(b)-Unstable\ OCs$	0/1000	241/1000	0/1000
$(b)-Cost\ reduction$	−3.2m (−53%)	−4.1m (−67%)	−3.7m (−62%)

system's response to the fault. The preventive curtailment of the wind power almost halved the unstable OCs, however both the approaches (i)-(ii) outperformed the WIND CURTAIL approach by making the system transient stable for all the studied 1000 load scenarios.

In terms of cost savings, approach (ii) decreased the cost of preventive control by 46% and 60% for scenario (a)-(b) compared to the WIND CURTAIL approach. Approach (i) based on the neural learning of the Lypaunov function further reduced these costs by 2%. The higher cost reduction when using approach (i) instead of approach (ii) confirmed that using the LQR controller to find the Lyapunov function did not allow to fully leverage the available storage capacity from EVs as the corresponding ROA and the consequent transient bounds significantly restricted the deviations in generation from the initial pre-fault OC. Therefore, a larger generation redispatch was considered to maintain the system transient stable resulting in an increase of the operating costs for preventive control.

C. Stability Analysis

In this study, three control approaches for cost-optimal transient stable operations were compared in terms of stability:

i) optimised PREVENTIVE CONTROL
ii) DT CONTROL, a decision tree based corrective control
iii) NN-LYAPUNOV CONTROL.

The PREVENTIVE CONTROL approach optimised the generation redispatch to guarantee transient stability using the Lyapunov based stability constraints, however no corrective control was applied. The DT CONTROL approach optimised only the generation redispatch as preventive control. However, no constraints for transient stability were considered in the optimisation problem. The stability of the optimised pre-fault OC was then assessed using a DT. When the OC was unstable, corrective control was used to reduce the difference in generation between this optimised OC and the closest stable one in terms of euclidean distance [37]. The proposed NN-LYAPUNOV CONTROL approach optimised preventive and corrective control to balance operating costs and system stability (9a)–(9r). Following the fault, TAMs were used for 0.15 s before the activation of corrective control in all approaches.

The stability results for these three approaches are summarised in Table II for scenarios (a)-(b). It resulted that the proposed NN-LYAPUNOV CONTROL outperformed the baseline approach in Table I and the DT CONTROL approach in Table II by reducing the instability rate by 42% and 10% for scenario (a) and by 51% and 24% for scenario (b). Although similar stability performance of the NN-LYAPUNOV CONTROL were expected when using the PREVENTIVE CONTROL approach as the same stability constraints were considered in the optimisation, the number of unstable OCs slightly increased for scenario (a) with PREVENTIVE CONTROL. This is because the use of only preventive control to transient stability increased the pre-fault generation so much to make the TAMs less effective, and hence increased the number of unstable OCs.

D. Quantifying the Value of Corrective Control

This study investigated the value of corrective control in terms of cost savings and CO2 emissions. The proposed control approach to transient stability combines preventive and corrective control to reduce the operating costs of preventive control and prevent wind power curtailment.

To quantify the cost benefits of actively using corrective control for system stability, the three approaches described in Section V-C were compared against the WIND CURTAIL approach with regards to the cost of preventive control. The cost results are summarised in Table II. As expected, the WIND CURTAIL approach resulted in the highest operational costs as fossil fuel generation replaced the curtailed wind power to meet the power balance and the cost of fossil fuel generation is much higher than wind power. However, the proposed NN-LYAPUNOV CONTROL reduced the costs by 48% and 62% for scenario (a) and (b), respectively, compared to the WIND CURTAIL approach as the optimised use of corrective control allowed preventing wind curtailment. Similarly, the optimised PREVENTIVE CONTROL resulted in a lower cost reduction than the corrective based approaches as no resources were available in addition to the preventive strategies to maintain the system transient stable. Although the DT CONTROL approach resulted in slightly higher reductions of the operating costs compared to the proposed NN-LYAPUNOV CONTROL, this approach cannot guarantee the same high stability performance of the proposed one. The key finding is that the NN-LYAPUNOV CONTROL proposed approach resulted in the best balance between system stability and operating costs for preventive control as shown in Fig. 6 (the proposed approach is in green).

To quantify carbon emissions, the proposed control approach prevented the curtailment of 128 MWh and 192 MWh of wind power for each unstable OC for scenario (a)-(b), respectively, corresponding to a reduction of 420 kg of CO2 emissions for each uncurtailed MWh. For scenario (b) with 40% of wind power

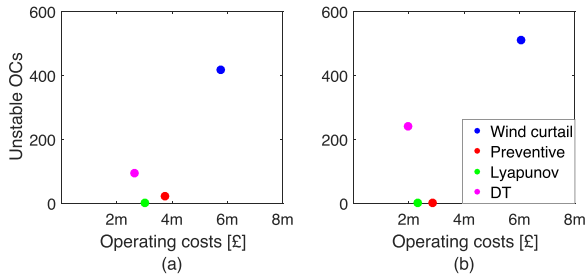

Fig. 6. The balance between stability and operating costs for four control approaches with 25% (a) and 40% (b) renewable integration.

TABLE III
STABILITY OF THREE CONTROL APPROACHES IN LARGE SYSTEMS

	Approaches		
	NO CONTROL	LQR CONTROL	LYAPUNOV CONTROL
$(c) - Unstable\ OCs$	$470/500$	$425/500$	$0/500$
$(d) - Unstable\ OCs$	$347/500$	$178/500$	$0/500$

generation and with the 99% of unstable OCs, the proposed approach reduced the CO2 emissions by up-to 80 m kg corresponding to the 60% of the total CO2 emissions when using WIND CURTAIL approach.

E. Performance on Larger Systems

In this study, the proposed approach was tested on the (c) IEEE 39-bus and (d) 118-bus systems. For the case study settings, the numerical error parameter was set at $\varepsilon = 0.5$ and $\delta = 0.01$ for the falsification step, so that the neural Lyapunov learning converged in 4668 and 9275 iterations for (c) and (d), respectively. The proposed NN-LYAPUNOV CONTROL was compared against i) the NO CONTROL approach when no preventive and corrective control was applied, and ii) the LQR-LYAPUNOV CONTROL where the stability constraints for the security-constrained OPF were derived from the initial LQR controller.

The stability results are summarised in Table III. There, the NN-LYAPUNOV CONTROL outperformed approaches (i)-(ii) by making the system transient stable for all the studied 500 load scenarios in both systems. This result demonstrates that enlarging the ROA can leverage the available EV storage capacity to improve the system stability in these larger systems.

The computational times of the proposed NN-LYAPUNOV CONTROL approach for different system sizes are also investigated. Two components need to be considered: i) computational time to learn the Lyapunov function; ii) computational time to solve the ACOPF. The learning times of the Lyapunov function for different systems are in [25], showing that training a NN for the IEEE 118-bus system can take around 45 min. Considerations with this long training time is part of the discussion section. The solver time for the SDP based ACOPF is only 2.1 s for each OC for the 118-bus system, but scales to 24 min for a 3375-bus system [31], that may be still an acceptable time when the fault is foreseen. Switching to use commercial solvers such as Mosek and developing advancements in operational research may likely reduce this computational time further.

F. Discussion

The proposed control approach optimally balances the cost of normal operation considering preventive and corrective control and the transient stability. This approach has a promising performance from several viewpoints. From the stability viewpoint, the NN-LYAPUNOV CONTROL reduced the unstable OCs by up-to 99% and 51% when not using control and when using preventive WIND CURTAIL approach, respectively. Although the stability performance of the proposed approach was comparable to the optimised PREVENTIVE CONTROL, the NN-LYAPUNOV CONTROL outperformed the other approaches with regards to normal operating costs by a reduction of up-to 62% when compared against the WIND CURTAIL approach. This is a key step forward to secure power system operations as the costs for renewable curtailment are generally very high, for example renewable curtailment costed € 372.7 m in Germany in 2016 corresponding to the 43% of the total cost for congestion management [38]. Only the DT CONTROL resulted in slightly lower operating costs. However, the cost of experiencing unstable OCs is much higher than the difference in the operating costs between the proposed approach and the DT CONTROL one. Therefore, the proposed approach resulted in the best balance between stability and operating costs. Importantly, the proposed NN-LYAPUNOV CONTROL approach reduced carbon emissions by 60% through avoiding the curtailment of wind.

The proposed control approach for transient stability still has a few limitations that need to be considered. The learning times for the stability constraints are quite high for larger systems. However, this learning step is carried out offline (Fig. 2) well ahead of real-time operation with no limitations on computational resources, and may only be done once (or in regular time intervals). The unforeseen fault scenario was not investigated in this work as no preventive control would be available for unexpected faults, and this work focuses on a cost-optimal combination of preventive and corrective tools. Training offline a NN to instantly predict the cost-optimal solution of the SDP based optimisation in real-time could be a potential research direction to investigate to improve the applicability of the proposed approach to real-time applications [6]. Only a NN model was tested to learn the controller and the Lyapunov function. However, the performance of such models were better discussed in [22] showing that it is worth using NNs for this task. Intuitively, larger NN models with larger numbers of layers and neurons would be needed for larger systems and this would increase the learning time [25]. Therefore, the trade-off between larger NN model's sizes and higher learning time should be also investigated. The performance of the proposed approach on future systems with higher shares of renewables than 40% should be also tested. Finally, relying on machine learning based control approaches rather than investing in new grid infrastructure or curtailing wind power in advance has a risk that should be considered in the decision making process.

VI. CONCLUSION

The need for novel operating methods to deal with the new dynamical phenomena was investigated showing that future

grids can suffer from highly unstable operations. In a scenario where renewable sources and DERs make the generation more uncertain and the demand more flexible and CIGs scale the timescale of interest down to a few milliseconds, fast corrective control methods available in real-time are needed. In response, a new real-time operating approach that utilises the high flexibility that DERs (EVs in this work) have to offer was proposed. The key advancement of this approach is that corrective control can be used in normal operation, not only as backup strategies when preventive control fails. The vision of this work is that corrective control actively participates in maintaining the system stability. The proposed approach optimises the combination of preventive and corrective applications to reduce the operating costs and carbon emissions, and enhance the system stability. Concluding from the studies on the IEEE 9-bus system with high shares of renewable generation and integrated DERs and on the IEEE 39-bus and 118-bus systems: the approach outperformed existing control approaches in balancing operating costs and stability, resulting in reductions of up to 62% and 51% for the costs and the number of unstable OCs. Also in a larger system, the approach resulted in high stability performance. This paper recommends considering the proposed method in a real operating tool, then, as this paper showed, a significant step forward could be made toward reducing wind curtailment and carbon emissions by upto 60%.

REFERENCES

[1] P. Panciatici, G. Bareux, and L. Wehenkel, "Operating in the fog: Security management under uncertainty," *IEEE Power Energy Mag.*, vol. 10, no. 5, pp. 40–49, Oct. 2012.

[2] F. Milano, F. Dörfler, G. Hug, D. J. Hill, and G. Verbič, "Foundations and challenges of low-inertia systems," in *Proc. IEEE Power Syst. Computation Conf.*, 2018, pp. 1–25.

[3] M. Panteli and P. Mancarella, "The grid: Stronger, bigger, smarter?: Presenting a conceptual framework of power system resilience," *IEEE Power Energy Mag.*, vol. 13, no. 3, pp. 58–66, May/Jun. 2015.

[4] R. Moreno, D. Pudjianto, and G. Strbac, "Transmission network investment with probabilistic security and corrective control," *IEEE Trans. Power Syst.*, vol. 28, no. 4, pp. 3935–3944, Nov. 2013.

[5] Y. Pipelzadeh, R. Moreno, B. Chaudhuri, G. Strbac, and T. C. Green, "Corrective control with transient assistive measures: Value assessment for Great Britain transmission system," *IEEE Trans. Power Syst.*, vol. 32, no. 2, pp. 1638–1650, Mar. 2017.

[6] N. Guha, Z. Wang, M. Wytock, and A. Majumdar, "Machine learning for AC optimal power flow," 2019, *arXiv:1910.08842*.

[7] R. Canyasse, G. Dalal, and S. Mannor, "Supervised learning for optimal power flow as a real-time proxy," in *Proc. IEEE Power Energy Soc. Innov. Smart Grid Technol. Conf.*, 2017, pp. 1–5.

[8] S. Abhyankar, G. Geng, M. Anitescu, X. Wang, and V. Dinavahi, "Solution techniques for transient stability-constrained optimal power flow–part I," *IET Generation, Transmiss. Distrib.*, vol. 11, no. 12, pp. 3177–3185, 2017.

[9] G. Geng, S. Abhyankar, X. Wang, and V. Dinavahi, "Solution techniques for transient stability-constrained optimal power flow–part II," *IET Generation, Transmiss. Distrib.*, vol. 11, no. 12, pp. 3186–3193, 2017.

[10] V. Miranda, J. N. Fidalgo, J. A. P. Lopes, and L. B. Almeida, "Real time preventive actions for transient stability enhancement with a hybrid neural network-optimization approach," *IEEE Trans. Power Syst.*, vol. 10, no. 2, pp. 1029–1035, May 1995.

[11] M. La Scala, M. Trovato, and C. Antonelli, "On-line dynamic preventive control: An algorithm for transient security dispatch," *IEEE Trans. Power Syst.*, vol. 13, no. 2, pp. 601–610, May 1998.

[12] Q. Jiang and Z. Huang, "An enhanced numerical discretization method for transient stability constrained optimal power flow," *IEEE Trans. Power Syst.*, vol. 25, no. 4, pp. 1790–1797, Nov. 2010.

[13] M. Pavella, D. Ernst, and D. Ruiz-Vega, *Transient Stability of Power Systems: A Unified Approach to Assessment and Control*. Berlin, Germany: Springer Science & Business Media, 2012.

[14] A. Michel, A. Fouad, and V. Vittal, "Power system transient stability using individual machine energy functions," *IEEE Trans. Circuits Syst.*, vol. 30, no. 5, pp. 266–276, May 1983.

[15] P. Varaiya, F. F. Wu, and R.-L. Chen, "Direct methods for transient stability analysis of power systems: Recent results," *Proc. IEEE*, vol. 73, no. 12, pp. 1703–1715, Dec. 1985.

[16] S. Izumi, H. Somekawa, X. Xin, and T. Yamasaki, "Estimation of regions of attraction of power systems by using sum of squares programming," *Elect. Eng.*, vol. 100, no. 4, pp. 2205–2216, 2018.

[17] T. L. Vu and K. Turitsyn, "Lyapunov functions family approach to transient stability assessment," *IEEE Trans. Power Syst.*, vol. 31, no. 2, pp. 1269–1277, Mar. 2016.

[18] P. Giesl and S. Hafstein, "Review on computational methods for Lyapunov functions," *Discrete Continuous Dynamical Syst.- Ser. B*, vol. 20, no. 8, pp. 2291–2331, 2015.

[19] V. Petridis and S. Petridis, "Construction of neural network based Lyapunov functions," in *Proc. IEEE Int. Joint Conf. Neural Netw. Proc.*, 2006, pp. 5059–5065.

[20] N. Noroozi, P. Karimaghaee, F. Safaei, and H. Javadi, "Generation of Lyapunov functions by neural networks," in *Proc. World Congr. Eng.*, vol. 2008, 2008, pp. 61–65.

[21] S. M. Richards, F. Berkenkamp, and A. Krause, "The lyapunov neural network: Adaptive stability certification for safe learning of dynamical systems," in *Proc. Conf. Robot Learn.*, 2018, pp. 466–476.

[22] Y.-C. Chang, N. Roohi, and S. Gao, "Neural lyapunov control," *Adv. Neural Inf. Process. Syst.*, vol. 32, 2019.

[23] W. Cui and B. Zhang, "Lyapunov-regularized reinforcement learning for power system transient stability," *IEEE Control Syst. Lett.*, vol. 6, pp. 974–979, 2022.

[24] T. Huang, S. Gao, X. Long, and L. Xie, "A neural lyapunov approach to transient stability assessment in interconnected microgrids," in *Proc. 54th Hawaii Int. Conf. System Sci.*, 2021, Art. no. 3330.

[25] T. Zhao, J. Wang, X. Lu, and Y. Du, "Neural Lyapunov control for power system transient stability: A. deep learning-based approach," *IEEE Trans. Power Syst.*, vol. 37, no. 2, pp. 955–966, Mar. 2022.

[26] P. M. Anderson and A. A. Fouad, *Power System Control and Stability*. Hoboken, NJ, USA: Wiley, 2008.

[27] G. Li and S. Rovnyak, "Integral square generator angle index for stability ranking and control," *IEEE Trans. Power Syst.*, vol. 20, no. 2, pp. 926–934, May 2005.

[28] B. Severino and K. Strunz, "Enhancing transient stability of DC microgrid by enlarging the region of attraction through nonlinear polynomial droop control," *IEEE Trans. Circuits Syst. I: Regular Papers*, vol. 66, no. 11, pp. 4388–4401, Nov. 2019.

[29] H. Kwakernaak and R. Sivan, *Linear Optimal Control Systems*, vol. 1. New York, NY, USA: Wiley-interscience, 1972.

[30] S. Gao, J. Avigad, and E. M. Clarke, "δ-Complete decision procedures for satisfiability over the reals," in *Proc. Int. Joint Conf. Automated Reasoning*, Springer, 2012, pp. 286–300.

[31] D. K. Molzahn, J. T. Holzer, B. C. Lesieutre, and C. L. DeMarco, "Implementation of a large-scale optimal power flow solver based on semidefinite programming," *IEEE Trans. Power Syst.*, vol. 28, no. 4, pp. 3987–3998, Nov. 2013.

[32] J. H. Chow, *Time-Scale Modeling of Dynamic Networks With Applications to Power Systems*, vol. 46. Berlin, Germany: Springer, 1982.

[33] A. Shakoor, G. Davies, G. Strbac, D. Pudjianto, F. Teng, and D. Papadaskalopoulos, "*Roadmap for Flexibility Services to 2030: A. Report to the Committee on Climate Change*," 2017.

[34] A. Paszke et al., "Pytorch: An imperative style, high-performance deep learning library," *Adv. Neural Inf. Process. Syst.*, vol. 32, pp. 8026–8037, 2019.

[35] J. Q. Tortós and V. Terzija, "Controlled islanding strategy considering power system restoration constraints," in *Proc. IEEE Power Energy Soc. Gen. Meeting*, 2012, pp. 1–8.

[36] D. P. Wadduwage, C. Q. Wu, and U. Annakkage, "Power system transient stability analysis via the concept of Lyapunov exponents," *Electric Power Syst. Res.*, vol. 104, pp. 183–192, 2013.

[37] I. Genc, R. Diao, V. Vittal, S. Kolluri, and S. Mandal, "Decision tree-based preventive and corrective control applications for dynamic security enhancement in power systems," *IEEE Trans. Power Syst.*, vol. 25, no. 3, pp. 1611–1619, Aug. 2010.

[38] M. Joos and I. Staffell, "Short-term integration costs of variable renewable energy: Wind curtailment and balancing in Britain and Germany," *Renewable Sustain. Energy Rev.*, vol. 86, pp. 45–65, 2018.